THE ASTROPHYSICAL JOURNAL, 513:69–75, 1999 March 1

A NEW ASSESSMENT OF THE COMPLETENESS OF QUASAR SURVEYS: IMPLICATIONS FOR THE LUMINOSITY FUNCTION

MATTHEW J. GRAHAM AND ROGER G. CLOWES
Centre for Astrophysics, University of Central Lancashire, Preston PR1 2HE, England, UK; m.j.graham, r.g.clowes@uclan.ac.uk

AND

LUIS E. CAMPUSANO
Observatorio Astronómico Cerro Calán, Departamento de Astronomía, Universidad de Chile, Casilla 36-D, Santiago, Chile; luis@das.uchile.cl
Received 1998 September 29; accepted 1998 October 6

ABSTRACT

We apply a simple statistical method to estimating the completeness of quasar surveys. It requires that an area has been covered by two or more, preferably different, selection techniques. We use three suitable data sets with separate selections from the following: variability and UV excess (170 quasars); objective prism and UV excess (141 quasars); and multicolor and X-ray (*ROSAT*, 19 quasars). We find that, for selection by UV excess, the common limit of $U-B \leq -0.35 \pm -0.05$ leads to losses of $\sim 35\%$, typically missing low-luminosity ($M_B \gtrsim -24.5$) quasars, independently of redshift. Systematic incompleteness will therefore affect the new generation of large quasar surveys that select by $U-B \leq -0.35$. By correcting for this incompleteness, we find from the first data set ($B < 21.0$ and $z < 2.2$) that the evolution of the quasar luminosity function (LF) is best described by joint luminosity and density evolution. When extrapolated to $z = 0$, the LF matches that of local Seyfert galaxies better than any previous determination. The LF shows an increase in the number of low-luminosity quasars at low redshifts and of brighter quasars at intermediate redshifts, relative to the 1990 LF of Boyle and coworkers. This result is consistent with models in which quasars fade from an initial bright phase.

Subject headings: galaxies: luminosity function, mass function — galaxies: Seyfert — surveys

1. INTRODUCTION

The completeness of a quasar survey should properly be specified by the survey selection function, $P(M, z, \mathrm{SED})$, which gives the probability of detecting a quasar as a function of absolute magnitude, redshift and spectral energy distribution (SED). The number of detected quasars in each cell of (M, z, SED) space is divided by $P(M, z, \mathrm{SED})$ to give the number of quasars that could be found. Summation over all cells gives the total population of quasars within the survey limits. In practice, $P(M, z, \mathrm{SED})$ cannot usually be determined reliably, and many cells may be empty or too poorly occupied for reliable estimates of the true number.

In this paper, we apply a statistical method to estimating the completeness of quasar surveys. It requires that an area of sky has been covered by two or more, preferably different, selection techniques. It does not require $P(M, z, \mathrm{SED})$.

We adopt $H_0 = 50$ km s^{-1} Mpc^{-1}, $q_0 = 0.5$, and $\alpha = 0.5$ ($f_\nu \propto \nu^{-\alpha}$).

2. ESTIMATING COMPLETENESS: THE METHOD

The method for estimating the completeness of a quasar survey involves the comparison of the number of detected quasars and an estimate of the total population. The total population is estimated using the method devised by Derenzo & Hildebrand (1969, hereafter DH) for estimating scanning efficiencies in the detection of events in particle physics. The use of the DH method here is appropriate, because in both applications the size of a total set of events is estimated from repeated scans of the set, with each scan yielding only a subset. In DH, the total number of particle events is estimated from repeated scans of film records; in this paper, the total number of quasar events is estimated from repeated scans (surveys) of an area of sky.

In a similar application to ours, Harwit & Hildebrand (1986) used the DH method to estimate the remaining number of observational phenomena still to be discovered in astronomy. Four kinds of scans were defined according to their usage of (1) optical continuum methods, (2) radio techniques, (3) optical spectroscopy, and (4) all other techniques to discover astronomical phenomena.

As a demonstration, we have applied the method to two samples of objects derived from a known parent population. We show that the total number of objects in the parent population is satisfactorily recovered.

The net visibility, v, of an object is defined to be the probability that it will be found by an *average* detection technique. It takes values ranging from 0 (invisible) to 1 (unmissable). Note that the net visibility depends on both the intrinsic characteristics of the object and the perceptiveness of the detection techniques.

The net visibility function, $F(v)$, is defined in such a way that $F(v)\,dv$ is the number of objects with net visibilities in the range v to $v + dv$. The total number of objects is then

$$N_T = \int_0^1 F(v)dv \; .$$

Note that $F(v)$ is an *average* of visibility functions for the individual techniques (DH). The existence of visibilities and visibility functions is an assumption of the method. See the Appendix for a formal derivation of $F(v)$ and the above result for N_T.

If all objects had equal prior probability of being detected, then $F(v)$ would be a δ function at the average detection probability. In general, however, $F(v)$ is an unknown function that must be estimated.

Consider a population that is surveyed using several techniques, preferably different but not necessarily. Suppose, for example, that there are three techniques. A first technique (A) detects A objects, another technique (B) detects B objects, and a third technique (C) detects C

objects. A particular object may be detected by more than one technique.

The average number of objects detected by one application of the average technique, $M[1]$, is the average number detected by the three techniques

$$M[1] = (A + B + C)/3 .$$

To determine the average number of new objects detected by the second application of the average technique, we take the techniques in pairs. A new object is detected if it is seen by one technique but not by the other. Thus

$$M[2] = [Ab + Ac + Ba + Bc + Ca + Cb]/6 ,$$

where Ab denotes the number of objects detected by technique A but missed by technique B and so forth. Similarly, the average number of new objects found by the third application of the average technique is

$$M[3] = [Abc + Bac + Cab]/3 .$$

In general, the distributions of undetected objects after one, two, and $i-1$ surveys are, respectively, $F(v)(1-v)$, $F(v)(1-v)^2$, and $F(v)(1-v)^{i-1}$. Hence the number of new objects found in the i^{th} survey using the average technique will be

$$M[i] = \int_0^1 vF(v)(1-v)^{i-1}\, dv . \qquad (1)$$

The collection of values $M[1]$, $M[2]$, ... , $M[n]$ can then be used to evaluate $F(v)$, if we assume for $F(v)$ an expression with not more than n parameters, where n is the number of surveys.

Harwit & Hildebrand (1986) argue that, in general, the total number of objects, N_T, derived from $F(v)$ will be approximately the same for any smooth trial function, $F(v)$, whose m parameters ($m \leq n$) are adjusted to give satisfactory fits to the values of $M[i]$. DH show that for any function $F(v)$ that is integrable in the region $0 \leq v \leq 1$ and for all values of $M[i]$, $i = 1, \ldots, \infty$ that satisfy equation (1), a lower limit for N_T is given by

$$N_T \geq \left(\sum_i^n M[i]\right) + \left(\frac{M^2[n]}{M[n-1]}\right)\left(1 - \frac{M[n]}{M[n-1]}\right)^{-1} ,$$

subject only to statistical fluctuations in the measured quantities $M[1]$, ... , $M[n]$.

In the case where $n = 2$, this expression can be rewritten as

$$N_T \geq \frac{(A \cup B + A \cap B)^2}{4(A \cap B)} .$$

This shows that, when there are only two surveying techniques, the estimated lower limit for N_T depends on the number of objects that both techniques have in common ($A \cap B$). When the total number of objects detected by both techniques is very large but the number of objects in common is relatively small, this dependency will lead to a very large estimate of N_T. From an analysis of the behavior of the above expression in these circumstances, we have found that unreliable estimates of N_T tend to be given when $(A \cup B)/(A \cap B) \gtrsim 5$. We therefore recommend that the method is applied only to data sets in which this ratio is $\lesssim 5$. There are no such discontinuities for higher values of n.

As a demonstration of the method, we consider the optical survey by Tritton & Morton (1984). They identified all objects in a region of 0.31 deg^2, finding 747 ordinary stars, 3 white dwarfs, 4 quasars, and 143 galaxies. We take the 601 stars found with $B \leq 20.0$ as a complete sample and then isolate two subsets by different selection criteria: (1) 379 stars with $B-V < 1.0$; (2) 312 stars with an objective-prism classification of spectral type earlier than K. Subset 1 has 111 stars not found in subset 2; subset 2 has 44 stars not found in subset 1. This gives $M[1] = 345.5$ and $M[2] = 77.5$, and hence $N_T \geq 445$. The trial functions used in the following sections give estimates of the total number in the range 445–667, which embraces the actual total of 601 stars. The median estimate is 546.

3. ESTIMATING COMPLETENESS: THE SURVEYS

The method estimates the total number of quasars in the parameter space defined by the boundaries of a data set; that is, the total number of quasars lying within the magnitude, redshift, and SED ranges of the data set. We have applied the method to three suitable data sets, each based on two different survey techniques but satisfying our condition that $(A \cup B)/(A \cap B) \lesssim 5$.

Data set 1 is based on a survey of quasars in ESO/SERC field 287 by Hawkins & Véron (1995) (see also: Hawkins & Véron 1993; Véron & Hawkins 1995). Quasar candidates were selected primarily by variability ($s > 3.5$, where s is a variability parameter typically 10 times the amplitude of the variability), although a UV-excess (UVX) criterion ($U-B < 0$) was also used. The survey actually consists of three samples: (1) a faint sample of 111 quasars covering 4.6 deg^2 with $19.5 < B < 21.0$ and $z < 2.2$; (2) a bright sample of 117 quasars covering 18.8 deg^2 with $B < 19.5$ and $z < 2.2$; and (3) a high-redshift sample of 86 quasars covering 18.8 deg^2 with $B < 21.0$ and $z > 2.2$. We construct data set 1 from the faint sample and those quasars from the bright sample that lie within the boundaries of the faint sample. It comprises 170 quasars covering 4.6 deg^2 with $B < 21.0$ and $z < 2.2$. We have not considered quasars with $z > 2.2$, because they were not sampled by two independent methods but were selected jointly on their color and variability. The intrinsic luminosity limit for data set 1 is $M_B = -19.83$; 145 quasars would be detected by their variability ($s > 3.5$) and 163 by their color ($U-B < 0$), giving $M[1] = 154$. Only seven quasars are found by variability that are not found by UVX, whereas UVX finds 25 quasars not detected by their variability, which gives $M[2] = 16$.

Data set 2 is based on two quasar surveys of ESO/SERC field 927: (1) a sparse-sampling survey of 118 quasars, selected by the Automated Quasar Detection software (AQD; Clowes 1986; Clowes, Cooke, & Beard 1984), covering 25 deg^2 with $B < 20.8$ and $z < 2.8$ (Clowes & Campusano 1994; Graham 1997; Clowes, Campusano, & Graham 1999); (2) a survey of 151 quasars, selected by UVX $U-BL-0.3$, covering 14.4 deg^2 with $B < 20.0$ and $z < 2.8$ (Graham 1997). Data set 2 is constructed from all the UVX-selected quasars with $z < 2.2$ and all the AQD-selected quasars with $B < 20$, $z < 2.2$ that lie within the boundaries of the UVX survey. It comprises 141 quasars in 14.4 deg^2 and has an intrinsic luminosity limit of $M_B = -21.04$; 135 quasars were found in the UVX survey, and 49 quasars were found in the AQD survey, satisfying the relevant criteria. Only six quasars were found by AQD that were not detected by UVX, whereas UVX found 92 quasars not detected by AQD. Thus $M[1] = 92$, and $M[2] = 49$.

Data set 3 is based on two surveys of selected area 57 (SA57): (1) a survey of 30 quasars selected by multicolor

techniques, covering 0.29 deg^2 with $B < 22.6$ and $z < 3.12$ (Koo & Kron 1988); (2) a survey of 19 quasars, selected from *ROSAT* HRI observations of SA57, covering 0.13 deg^2 with a limiting flux of 0.2×10^{-14} ergs s^{-1} cm^{-2} and $z < 3.02$ (Miyaji et al. 1997). Data set 3 is constructed from all *ROSAT*-selected quasars and all quasars from Koo & Kron that lie within 12′ of the *ROSAT* pointing center. It comprises 19 quasars covering 0.13 deg^2; 17 quasars were identified by Koo & Kron that meet the relevant criteria, and 19 were identified by *ROSAT*. No quasars were found by Koo & Kron that were not found by *ROSAT*, and two were found by *ROSAT* that were not found by Koo & Kron. Thus $M[1] = 18$, and $M[2] = 1$. Note, however, that of the 33 sources detected by *ROSAT* in SA57, seven are classed as faint stellar objects. These could be quasars, but they would be fainter than the magnitude limit of $B_J = 22.5$ of Koo & Kron (T. Miyaji 1997, private communication).

We have used the values of $M[1]$ and $M[2]$ for the three data sets to fit different trial functions, $F(v)$. The $F(v)$ and the corresponding estimates of the total number of quasars are given in Table 1. The figure in parentheses after each estimate is the completeness of the data set based on the estimated total number for the data set. The lower limit to the total number of quasars is also given. With two techniques contributing to a data set, the trial functions have only two free parameters. However, the trial functions give a good coverage of the possible functional forms of the true visibility function.

The estimates show that data set 1 is 63%–99% complete, data set 2 is 47%–72% complete, and data set 3 is 61%–100% complete. If we use the median estimates then data set 1 is 89% complete, data set 2 is 54% complete, and data set 3 is 90% complete. If we assume that there were errors of $(N)^{1/2}$ in the numbers of common (A, B) and distinct (Ab, Ba) objects comprising each survey, then the typical error in the estimate of the total number of objects is $\sim$5% in data set 1, $\sim$5% in data set 2, and $\sim$15% in data set 3.

The success rates for median estimates of the individual selection techniques are as follows: variability (with $s > 3.5$) selects 76%, and UVX (with $U-B < 0$) selects 86% of the total population of quasars for data set 1; UVX (with $U-B \leq -0.3$) selects 52%, and AQD selects 19% of the total for data set 2 (the AQD survey is by sparse sampling); and color selection finds 81%, and X-ray finds 90% of the total for data set 3.

4. COMMENTS ABOUT SURVEYS

Random incompleteness—effectively sparse sampling—does not affect the expectation values of any statistics if the sampling rate is known (Kaiser 1986). However, systematic incompleteness (e.g., bias against the detection of low-redshift or low-luminosity quasars) means that a sample is nonrandom, and incorrect conclusions may be drawn.

Samples of quasars selected by UVX ($U-B \leq -0.35 \pm 0.05$) are normally assumed, following Véron (1983), to contain at least 90% of the quasars with $z < 2.2$ within a given survey. However, our results suggest that a large fraction of quasars with $z < 2.2$, possibly as high as 50% (from data set 2), do not have a large UVX and must have been missed by previous UVX surveys, e.g., Boyle et al. (1990). Such losses could have serious consequences if the incompleteness is systematic. We can test for systematic incompleteness by examining the effectiveness of selection by UVX for different $U-B$ limits. To do this, we take data set 1 and consider UVX limits of $U-B \leq -0.35$ and $U-B \leq 0.0$.

One possibility is that a limit of $U-B \leq -0.35$ is biased against low-redshift quasars ($z < 0.7$). A plot of $U-B$ against redshift for all quasars in data set 1 suggests that this is likely (see Hawkins & Véron 1995, their Fig. 1). For data set 1, Table 1 shows the effectiveness of selection by UVX for $z > 0.7$. The figure in parentheses after each estimate is the effectiveness of selection by UVX with the relevant UVX limit. The lower limit to the total number of quasars present is also given. If only low-redshift quasars were being missed for $U-B \leq -0.35$, then for $z > 0.7$ the effectiveness for the two UVX limits should be approximately the same. This is clearly not the case.

A second possibility is that a limit of $U-B \leq -0.35$ is biased against low-luminosity quasars. Several authors

TABLE 1

DATA SETS ANALYZED AND RESULTS

PARAMETER	DATA SET 1	DATA SET 2	DATA SET 3	DATA SET 1			
				Subset 1 ($z > 0.7$)		Subset 2 ($M_B \leq -24.5$)	
Detection technique.....	UVX (0): 163 Var.: 145	UVX (−0.3): 135 AQD: 49	Color: 17 X-ray: 19	UVX (0): 125 Var.: 117	UVX (−0.35): 98 Var.: 117	UVX (0): 60 Var.: 55	UVX (−0.35): 55 Var.: 55
$M[1]$	154	92	18	122.5	108.5	57.5	55
$M[2]$	16	49	1	8.5	18.5	4.5	5
Number of quasars	170	141	19	131	127	62	60
	Trial functions $F(v) =$						
$K(1-av)$, $v < a^{-1}$	258 (66%)	295 (48%)	29 (66%)	198 (63%)	197 (50%)	94 (64%)	91 (60%)
0, $v \geq a^{-1}$	...	...	...	...	...	...	...
$K(1-v)^a$	190 (89%)	302 (47%)	21 (90%)	141 (89%)	154 (64%)	67 (90%)	66 (83%)
$K \exp(-av^2)$	271 (63%)	198 (71%)	31 (61%)	214 (58%)	219 (45%)	100 (60%)	96 (57%)
$K\delta(v-a)$.....	172 (99%)	197 (72%)	19 (100%)	132 (95%)	131 (75%)	62 (97%)	61 (90%)
K, $v < a$	171[a] (99%)	262 (54%)	18[a] (...)	176 (71%)	175 (56%)	60[a] (100%)	59[a] (93%)
0, $v \geq a$	...	...	...	...	...	...	...
Lower limit	172 (99%)	197 (72%)	19 (100%)	132 (95%)	131 (75%)	62 (97%)	61 (90%)

[a] Solution has $a > 1$; this is the value for $\int_0^1 F(v)\,dv$ (i.e., the upper limit is 1 and not a).

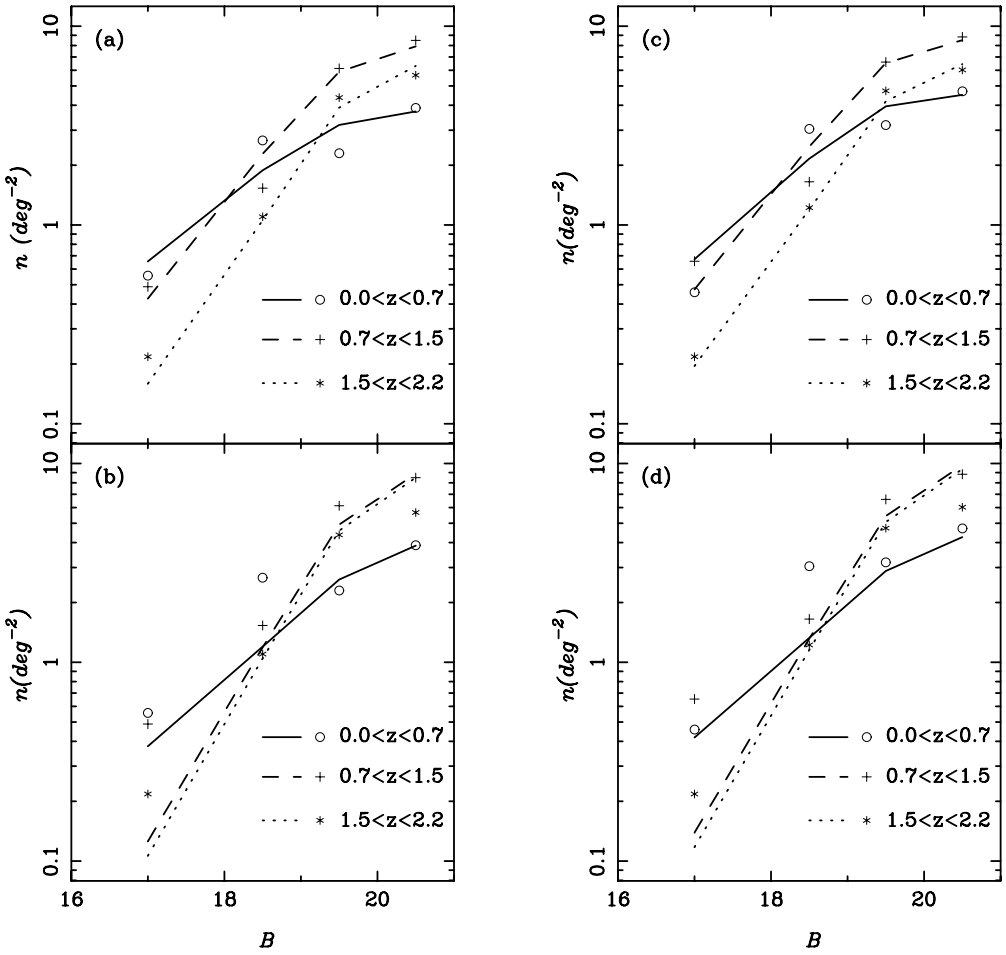

FIG. 1.—"True" surface density of quasars estimated in the various joint apparent magnitude and redshift bins using the maximum (*a*, *b*) and median (*c*, *d*) completeness estimators. The top panel for each estimated data set shows the predicted surface density using our best-fit LF model, and the bottom panel shows that predicted by model B from Boyle et al. (1990), normalized appropriately.

have considered such a bias as likely but estimate the incompleteness at ~10% (e.g., Boyle et al. 1990). Note that a survey that arbitrarily defines a quasar to have $M_B \leq -23$ (Schmidt & Green 1983) would also be biased against low-luminosity quasars. For data set 1, Table 1 similarly shows the effectiveness of selection by UVX for $M_B \leq -24.5$. If only low-luminosity quasars were being missed for $U-B \leq -0.35$, then for $M_B \leq -24.5$ the effectiveness for the two UVX limits should be approximately the same. This is indeed the case.

In summary, a quasar sample selected by $U-B \leq -0.35$ is systematically incomplete, being biased in particular against low-luminosity quasars. Part of the incompleteness is probably caused by detectable radiation from the host galaxy. This will redden the quasar, and it will cause losses in surveys that require candidates to be classified as starlike.

From the Parkes flat-spectrum quasars, Francis et al. (1997) have suggested the existence of three categories: (1) conventional blue quasars (40%); (2) red quasars, with reddening from synchrotron radiation (30%); and (3) very red quasars, with reddening from dust (30%). These last two categories of red quasars, being faint in *B*, could be the type of objects that comprise the low-luminosity population suggested by our analysis.

The incompleteness revealed by this work has implications for some of the new generation of large quasar surveys. For illustration, consider the AAT 2dF quasar survey (Smith et al. 1997). This currently specifies $U-B \leq -0.36$ and $18.25 < B < 21.0$, and it has a projected final completeness of ~90%. Adapting data set 1 to have the same selection criteria gives $M[1] = 124$ and $M[2] = 29.5$. The corresponding lower limit to the total number of quasars is $N_T \geq 163$, and the median value of the five estimators is 217; 104 quasars are detected with $U-B \leq -0.36$. Thus our results imply that, at best, the AAT 2dF survey will select only 64% of all quasars with $18.25 < B < 21.0$ and $z < 2.2$.

5. THE LUMINOSITY FUNCTION REVISITED

Previous determinations of the quasar luminosity function (LF) could have significantly underestimated the density of low-luminosity quasars. We can now estimate the incompleteness, correct for it, and so determine the "true" LF.

For data set 1, we have divided the ranges of apparent magnitude and redshift into bins: $16 < B \leq 18$, $18 < B \leq 19$, $19 < B \leq 20$, and $20 < B \leq 21$; $0 < z \leq 0.7$, $0.7 < z \leq 1.5$, and $1.5 < z \leq 2.2$. Within each joint magnitude and redshift bin, we have estimated the "true" surface density of quasars using both the maximum completeness estimator, $F(v) = K\delta(v-a)$, and the median completeness estimator, $F(v) = K(1-v)^a$. We have generated "best-fit"

models to these data using maximum likelihood techniques for various parametric forms for the LF. We consider two models involving pure luminosity evolution with parametric forms given by Boyle, Shanks, & Peterson (1988): a smoothed double power-law function,

$$\Phi(M, z) = \frac{\Phi^*}{10^{0.4[M - M(z)](\alpha+1)} + 10^{0.4[M - M(z)](\beta+1)}},$$

and a single power-law function,

$$\Phi(M, z) = \frac{\Phi^*}{10^{0.4[M - M(z)](\alpha+1)}},$$

where in both cases the redshift dependence, $M(z)$, can be expressed either as a $(1 + z)$ power-law evolution, $M(z) = M^* - 2.5k_L \log(1 + z)$, or as an exponential evolution with look-back time, $M(z) = M^* - 1.08k_L\tau$. The look-back time expressed as a fraction of the age of the universe is $\tau(z) = 1 - (1 + z)^{-3/2}$; Φ^* is a normalization factor.

We consider also a model with density and luminosity evolution parameterized as

$$\Phi(M, z) = \frac{\Phi^*\rho_D(z)}{10^{0.4[M - M(z)](\alpha+1)} + 10^{0.4[M - M(z)](\beta+1)}},$$

where the density evolution function is expressed as an exponential with look-back time

$$\rho_D(z) = \exp(k_D\tau) ;$$

α, β, M^*, k_L, and k_D are the free parameters that determine the fit.

The maximum likelihood solution is found in each case by minimizing the function:

$$S = -2\sum_{i,j} x_{ij} \log_e \mu_{ij} + 2\sum_{i,j} \mu_{ij},$$

where x_{ij} is the observed surface density in magnitude bin i and redshift bin j, μ_{ij} is the expected surface density in bin i and bin j, and the summation is over all bins.

Each best-fit model was tested for goodness of fit using the Pearson χ^2 statistic. Table 2 gives the best-fit parameters for the models and their χ^2 probabilities, $P(>\chi^2)$. For comparison, we have calculated how well some of the best-fit models of Boyle et al. (1990), normalized appropriately, fitted the data; these are also included in Table 2.

We can reject a single power-law LF and all of the best-fit models of Boyle et al. (1990). Of the remaining models, all of which incorporate double power-law LFs, the data are well described by those with density evolution. The best fits are obtained when all evolution is expressed by exponentials with look-back time. Figure 1 shows our best-fit models applied to the data; for comparison, the best-fit model of Boyle et al. (1990; model B), normalized appropriately, is also shown. At low redshifts the Boyle et al. model underestimates the number of faint quasars, and at intermediate redshifts it underestimates the number of brighter quasars. Figure 2 shows the LF corresponding to our best-fit model extrapolated to $z = 0$. For comparison the figure also shows the LF derived from local Seyfert galaxies of types 1 and 1.5 (Cheng et al. 1986); the LF for soft-X-ray–selected active galactic nuclei (AGNs; Franceschini et al. 1994), extrapolated to $z = 0$; and the Boyle et al. model B, extrapolated to $z = 0$. Our model provides the best-fit to the local Seyferts. The curve for X-ray–selected AGNs (including all types) lies a factor of ~ 2 above our LF, which suggests that other

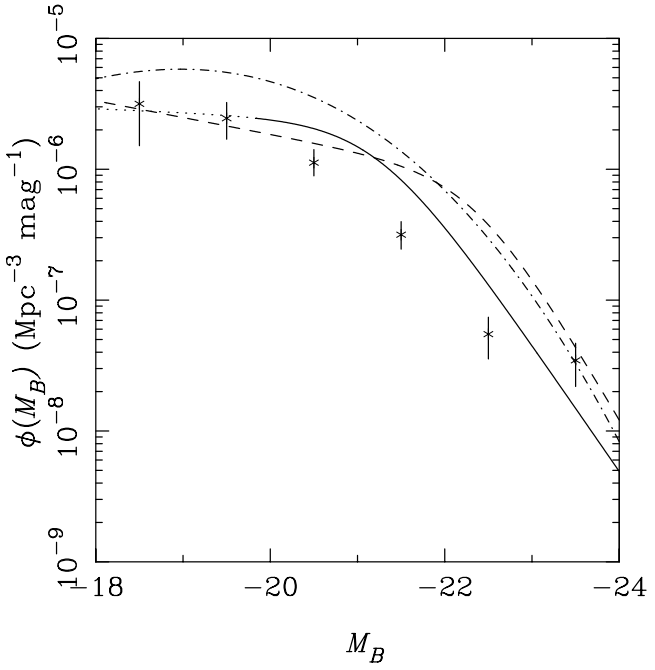

FIG. 2.—Quasar LF based on our best-fit model (*solid line*), extrapolated to $z = 0$, and the LF for Seyfert galaxies (Cheng et al. 1986; *asterisks*). The dotted line indicates the extrapolation of the quasar LF to magnitudes fainter than the limiting magnitude of the survey. The dashed line is model B from Boyle et al. (1990), extrapolated to $z = 0$, and the dot-dashed line is the LF for soft-X-ray–selected AGNs (Franceschini et al. 1994), extrapolated to $z = 0$.

TABLE 2

BEST-FIT PARAMETERS FOR EVOLUTIONARY MODELS

		α		β		M^*		k_L		k_D		$P(\chi^2)$	
LUMINOSITY MODEL	EVOLUTION	Max	Med	Max	Med	Max	Med	Max	Med	Max	Med	Max	Med
2 power law	$(1 + z)^{k_L}$	−3.50	−3.51	−1.24	−1.33	−23.38	−23.60	2.29	2.20	...	...	0.8732	0.7087
2 power law	$e^{k_L\tau}$	−3.56	−3.56	−1.26	−1.35	−22.26	−22.51	4.32	4.12	...	...	0.8572	0.6721
1 power law	$(1 + z)^{k_L}$	−1.83	−1.83	...	...	−22.71	−22.99	2.93	2.73	...	...	0.0048	0.0033
1 power law	$e^{k_L\tau}$	−1.85	−1.84	...	...	−16.62	−21.39	5.15	4.72	...	...	0.0078	0.0040
2 power law	$(1 + z)^{k_L}$	−3.35	−3.15	−1.00	−0.86	−22.51	−21.97	2.95	3.36	−1.06	−1.79	0.9385	0.9064
2 power law	$e^{k_L\tau}$	−3.42	−3.33	−1.07	−1.00	−21.23	−20.75	5.39	5.92	−1.08	−1.72	0.9392	0.9391
Boyle model B	$(1 + z)^{k_L}$	−3.87	−3.87	−1.32	−1.32	−22.37	−22.37	3.20	3.20	...	...	0.0410	0.0041
Boyle model M.....	$(1 + z)^{k_L}$	−3.90	−3.90	−1.34	−1.34	−22.59	−22.59	3.01	3.01	0.69	0.69	0.0162	0.0008
Boyle model N	$(1 + z)^{k_L}$	−3.89	−3.89	−1.29	−1.29	−22.79	−22.79	2.78	2.78	1.70	1.70	0.0006	4×10^{-6}

NOTE.—Parameters are derived using maximum (max) and median (med) completeness estimators.

types of AGN (e.g., starburst galaxies) are not related to quasars.

Compared with the most successful model of Boyle et al. (1990; model B), our LF shows an increase in the number of low-luminosity quasars at low redshifts and of brighter quasars at intermediate redshifts. It also matches well the LF of local Seyfert galaxies. Such behavior is consistent with quasar models in which evolution is caused by the progressive exhaustion of the fuel supply to the central black hole. Quasars fade from an initial bright phase until a low, quasi-steady rate of energy production is reached. This rate declines only slowly over a long timescale. Quasars in this final phase of evolution are equivalent to local Seyfert galaxies.

The referee provided helpful comments. M. J. G. acknowledges the support and hospitality of Departimento d'Astronomia i Astrofísica at the Universitat de Valencia. We thank T. Miyaji for providing us with data before their publication. L. E. C. was partially supported by FONDECYT grant 1970735.

APPENDIX

In this Appendix, we show that the total number of objects can be obtained from an average visibility function.

Consider a data set that is scanned N times. Each scan has its own visibility function, $f_i(v)$. Let X_i denote the number of objects found by scan i and x_i be the number of objects not found by scan i; then, for example, the expression $X_i x_j x_k$ represents the number of objects found by scan i but not by scan j or scan k.

Consider the average number of objects found in one scan:

$$M[1] = \frac{1}{N} \sum_i^N X_i \, .$$

In terms of the visibility function for a scanner,

$$X_i = \int_0^1 v f_i(v) dv \, ,$$

and so

$$M[1] = \frac{1}{N} \sum_i^N \int_0^1 v f_i(v) dv = \frac{1}{N} \int_0^1 v \sum_i^N f_i(v) dv \, .$$

If we define the average visibility function by

$$F(v) = \frac{1}{N} \sum_i^N f_i(v) \, ,$$

then

$$M[1] = \int_0^1 v F(v) dv \, .$$

Now consider the average number of new objects found in the second scan:

$$M[2] = \frac{1}{N(N-1)} \sum_{i,\, j(i \neq j)}^N X_i x_j \, .$$

For a single scanner (fixed i),

$$\frac{1}{N-1} \sum_{j(j \neq i)}^N X_i x_j = \int_0^1 v f_i(v)(1-v) dv \, ,$$

and so

$$M[2] = \frac{1}{N} \sum_i^N \int_0^1 v f_i(v)(1-v) dv = \frac{1}{N} \int_0^1 v \sum_i^N f_i(v)(1-v) dv = \int_0^1 v F(v)(1-v) dv \, .$$

In general, the average number of new objects found in the i^{th} scan will be

$$M[i] = \frac{1}{N(N-1) \ldots (N-i+1)} \sum_{i,\, j,\, \ldots,\, k(i \neq j \neq \ldots \neq k)}^N X_i x_j \ldots x_k \, .$$

For a single scanner (fixed i),

$$\frac{1}{(N-1) \ldots (N-i+1)} \sum_{j,\, \ldots,\, k(j \neq \ldots \neq k \neq i)}^N X_i x_j \ldots x_k = \int_0^1 v f_i(v)(1-v)^{i-1} dv \, ,$$

and so

$$M[i] = \int_0^1 vF(v)(1 - v)^{i-1}\, dv \ .$$

Now consider the integral,

$$\int_0^1 F(v)\, dv = \frac{1}{N} \int_0^1 \sum_i^N f_i(v) dv = \frac{1}{N} \sum_i^N \int_0^1 f_i(v) dv = N_T \ .$$

Thus, fitting an average visibility function to the data allows the total number of objects to be estimated.

REFERENCES

Boyle, B. J., Fong, R., Shanks, T., & Peterson, B. A. 1990, MNRAS, 243, 1
Boyle, B. J., Shanks, T., & Peterson, B. A. 1988, MNRAS, 235, 935
Cheng, F. Z., Danese, L., de Zotti, G., Franceschini, A. 1986, MNRAS, 212, 857
Clowes, R. G. 1986, Mitt. Astron. Ges., 67, 174
Clowes, R. G., & Campusano, L. E. 1994, MNRAS, 266, 317
Clowes, R. G., Campusano, L. E., & Graham, M. J. 1999, in preparation
Clowes, R. G., Cooke, J. A., & Beard, S. M. 1984, MNRAS, 207, 99
Derenzo, S. E., & Hildebrand, R. H. 1969, Nucl. Instrum. Methods Phys. Res., 69, 287
Franceschini, A., La Franca, F., Cristiani, S., & Martin-Mirones, J. M. 1994, MNRAS, 269, 683
Francis, P., Webster, R., Drinkwater, M., Masci, F., & Peterson, B. 1997, AAO Newsl. No. 82, 4
Graham, M. J. 1997, Ph.D. thesis, Univ. Central Lancashire
Harwit, M., & Hildebrand, R. 1986, Nature, 320, 724
Hawkins, M. R. S., & Véron, P. 1993, MNRAS, 260, 202
———. 1995, MNRAS, 275, 1102
Kaiser, N. 1986, MNRAS, 219, 785
Koo, D. C., & Kron, R. G. 1988, ApJ, 325, 92
Miyaji, T., Connolly, A. J., Szalay, A. S., & Boldt, E. 1997, A&A, 323, L37
Schmidt, M., & Green, R. F. 1983, ApJ, 269, 352
Smith, R. J., Boyle, B. J., Shanks, T., Croom, S. M., Miller, L., & Read, M. 1997, in IAU Symp. Proc. 179, New Horizons from Multiwavelength Sky Surveys, ed. B. J. McLean, D. A. Golombeck, J. J. E. Hayes, & E. Payne (Dordrecht: Kluwer), 348
Tritton, K. P., & Morton, D. C. 1984, MNRAS, 209, 429
Véron, P. 1983, in Quasars and Gravitational Lenses (Liége: Institut d'Astrophysique), 210
Véron, P., & Hawkins, M. R. S. 1995, A&A, 296, 665